Kinetics and Mechanism of Nucleophilic Substitutions on Coordinated Polyenes and Polyenyls. 1. Reactions of Tertiary Phosphines with $[Ru(\eta^5\text{-}C_5H_5)(\eta^4\text{-}C_5H_4O)(L)]CF_3SO_3$ (L = CH_3CN, Benzonitrile, Thiourea, Pyridine)

Walter Simanko,[1a] Thomas Vallant,[1a] Kurt Mereiter,[1b] Roland Schmid,[1a] and Karl Kirchner*,[1a]

Institute of Inorganic Chemistry and Institute of Mineralogy, Crystallography, and Structural Chemistry, Technical University of Vienna, Getreidemarkt 9, A-1060 Vienna, Austria

John Coddington[2] and Scot Wherland*,[2]

Department of Chemistry, Washington State University, Pullman, Washington 99164-4630

Received April 9, 1996[⊗]

Complexes of the type $[Ru(\eta^5\text{-}C_5H_5)(\eta^4\text{-}C_5H_4O)(L)]CF_3SO_3$ (L = CH_3CN (**1a**), benzonitrile (**1b**), pyridine (**2**), thiourea (**3**)) react with tertiary phosphines to give either 1,1′- or 1,2-disubstituted ruthenocenes depending on the basicity of the entering phosphine and the nature of L. For **1a** and **1b**, only phosphines with a pK_a value above 5 substitute on the C_5H_5 ring while others substitute on the C_5H_4O ring. For compounds **2** and **3**, the two rings are deactivated such that only the most basic phosphines react, and they attack only the C_5H_4O ring. In some cases of the reactions of **2** and **3**, an intermediate is observed in which the monodentate ligand has migrated to the C_5H_5 ring while the entering nucleophile coordinates to the metal center. The mechanism by which phosphines attack a coordinated C_5H_4O ring has been established, and detailed kinetic parameters have been obtained. For the reaction of **1a** with PPh_3, PPh_2Me, and P(*p*-PhOMe)$_3$ in acetone, the kinetics give a rate law indicating the reversible formation of an intermediate which goes irreversibly to the 1,2-disubstituted ruthenocene product. All three rate constants and their thermal activation parameters have been obtained for each of these reactions. For the P(p-PhOMe)$_3$ reaction, the volume of activation for each step has also been determined. The reaction of **2** and **3** with PBu^n_3, PCy_3, $PPhMe_2$, and PMe_3 in CD_3CN give a long-lived intermediate which also goes to the 1,2-disubstituted ruthenocene product. For the intermediates formed from **3**, the kinetics of this last step have been studied to determine the rate constants and their thermal activation parameters. In the case of PBu^n_3, the intermediate formed from **3** has been isolated and an X-ray structure determined, establishing that phosphine attack has occurred at the C_5H_4O ring.

Introduction

Organometallic ruthenium complexes containing the rarely used coligand cyclopentadienone (C_5H_4O) have recently attracted much of our attention.[3,4] In complexes of the type $[Ru(\eta^5\text{-}C_5H_5)(\eta^4\text{-}C_5H_4O)(L)]^+$, C_5H_4O is subject to nucleophilic attack by tertiary phosphines at a terminus of the coordinated 1,3-diene moiety to give, when L = CH_3CN, 1,1′-disubstituted complexes such as $[Ru(\eta^5\text{-}C_5H_5)(\eta^5\text{-}C_5H_4OH\text{-}2\text{-}PR_3)]^+$.[3-5] Most noteworthy, in addition to this simple diene reactivity, C_5H_4O is able to accept $2e^-$ and a proton while remaining coordinated as hydroxocyclopentadienide. This special feature of C_5H_4O effectively results in C−H activation of $C_5H_5^-$ and leads to nucleophilic attack by tertiary phosphines to give, from $[Ru(\eta^5\text{-}C_5H_5)(\eta^4\text{-}C_5H_4O)(CH_3CN)]^+$ (**1a**) or $[Ru(\eta^5\text{-}C_5H_5)(\eta^4\text{-}C_5H_4O)]_2^{2+}$, 1,2-disubstituted products such as $[Ru(\eta^5\text{-}C_5H_4\text{-}PMe_3)(\eta^5\text{-}C_5H_5OH)]^+$ (**7**).[3] Whether the product of nucleophilic attack is a 1,1′- or a 1,2-disubstituted ruthenocene is controlled by the entering phosphine and the ligand L, as depicted in Scheme 1.

A preliminary explanation for these unusual reactivity patterns has been given in terms of a strong resonance interaction of the C_5H_4O ligand with the ruthenium center.[3c] This explanation, however, considers only ground state stabilization. On a more rigorous basis, the electronic stabilization of the activated complex must be taken into account and in particular the change in electronic structure during the process of activation. For this purpose kinetic investigations are necessary in order to gain further insight into what appear to be elementary steps of organometallic reactions. Herein we report on the kinetics and mechanism of nucleophilic addition and substitution reactions of tertiary phosphines to $[Ru(\eta^5\text{-}C_5H_5)(\eta^4\text{-}C_5H_4O)(L)]CF_3SO_3$ complexes, where L = CH_3CN, benzonitrile, pyridine, and thiourea. In particular, we have now obtained kinetic data for the reactions that lead to 1,2-disubstituted products as well as a crystal structure of the intermediate in one such case.

Experimental Section

General Information. Manipulations were performed under an inert atmosphere of nitrogen by using standard Schlenk techniques and/or a glovebox. All chemicals were standard reagent grade and used without

⊗ Abstract published in *Advance ACS Abstracts,* September 1, 1996.

(1) (a) Institute of Inorganic Chemistry. (b) Institute of Mineralogy, Crystallography, and Structural Chemistry.
(2) Department of Chemistry, Washington State University.
(3) (a) Kirchner, K.; Taube, H. *J. Am. Chem. Soc.* **1991**, *113*, 7039. (b) Kirchner, K.; Taube, H.; Scott, B.; Willett, R. D. *Inorg. Chem.* **1993**, *32*, 1430. (c) Kirchner, K.; Mereiter, K.; Schmid, R.; Taube, H. *Inorg. Chem.* **1993**, *32*, 5553. (d) Kirchner, K.; Mereiter, K.; Mauthner, K.; Schmid, R. *Inorg. Chim. Acta* **1994**, *217*, 203. (e) Mauthner, K.; Mereiter, K.; Schmid, R.; Kirchner, K. *Organometallics* **1994**, *13*, 5054.
(4) Mauthner, K.; Slugovc, C.; Mereiter, K.; Schmid, R.; Kirchner, K. *Organometallics* **1996**, *15*, 181.
(5) Liebeskind, L. S.; Bombrun, A. *J. Am. Chem. Soc.* **1991**, *113*, 8736.

S0020-1669(96)00383-7 CCC: $12.00

Scheme 1

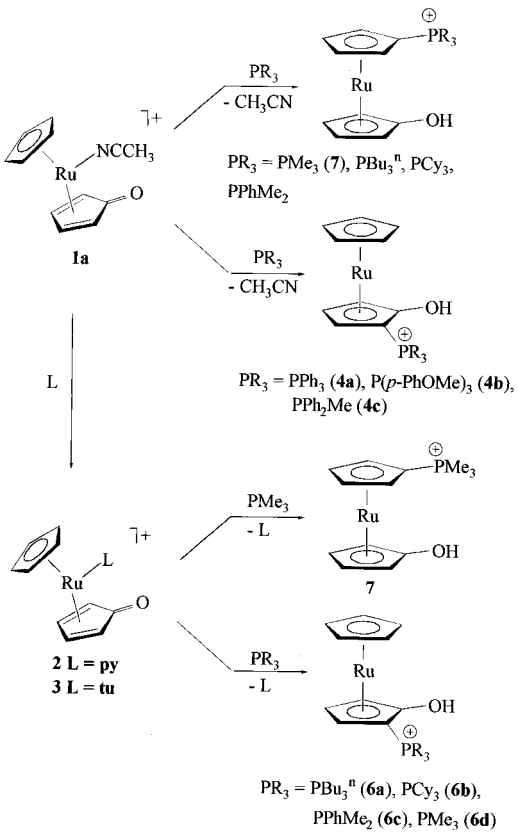

further purification. The solvents were purified according to standard procedures.[6] The deuterated solvents were purchased from Aldrich and dried over 4 Å molecular sieves. $[Ru(\eta^5\text{-}C_5H_5)(\eta^4\text{-}C_5H_4O)(CH_3CN)]CF_3SO_3$ (**1a**),[3a] $[Ru(\eta^5\text{-}C_5H_5)(\eta^4\text{-}C_5H_4O)(bn)]CF_3SO_3$ (bn = benzonitrile) (**1b**),[3b] $[Ru(\eta^5\text{-}C_5H_5)(\eta^4\text{-}C_5H_4O)(py)]CF_3SO_3$ (py = pyridine) (**2**),[3b] and $[Ru(\eta^5\text{-}C_5H_5)(\eta^4\text{-}C_5H_4O)(tu)]CF_3SO_3$ (tu = thiourea) (**3**)[3b] were prepared according to the literature. Infrared spectra were recorded on a Perkin-Elmer 16PC FTIR spectrometer. ^1H and $^{31}P\{^1H\}$ NMR spectra were recorded on a Bruker AC 250 spectrometer operating at 250.13 and 101.26 MHz, respectively, and were referenced to residual solvent protons and to PPh_3. Microanalyses were carried out by the Microanalytical Laboratories, University of Vienna.

Reaction of 1a with PPh_3 in CD_3NO_2. A 5 mm NMR tube was charged with **1a** (30 mg, 0.069 mmol) and capped with a septum. A solution of PPh_3 (1.5 equiv) in CD_3NO_2 (0.5 mL) was added by syringe, and the sample was transferred to an NMR probe. A ^1H NMR spectrum was immediately recorded. Characteristic resonances were observed at 2.58, 2.61, and 1.99 ppm assigned to coordinated CH_3CN of **1a**, coordinated CH_3CN of an intermediate, and liberated CH_3CN, respectively. After about 60 s, only resonances of free CH_3CN and $[Ru(\eta^5\text{-}C_5H_5)(\eta^5\text{-}C_5H_4OH\text{-}2\text{-}PPh_3)]CF_3SO_3$ (**4a**) were observed. In an analogous fashion, a $^{31}P\{^1H\}$ NMR spectrum was recorded showing, in addition to the signals of free PPh_3, resonances at 30.2 and 27.7 ppm indicating the formation of an intermediate and **4a**, respectively.

Reaction of 1b with PPh_3 in Acetone-d_6. A 5 mm NMR tube was charged with **1b** (30 mg, 0.060 mmol) and capped with a septum. A solution of PPh_3 in acetone-d_6 (0.5 mL) was added by syringe, and the sample was transferred to an NMR probe. A ^1H NMR spectrum was immediately recorded showing the formation of $[Ru(\eta^5\text{-}C_5H_5)(\eta^3\text{-}C_5H_4O\text{-}2\text{-}PPh_3)(bn)]CF_3SO_3$ (**5**). ^1H NMR (δ, acetone-d_6, 20 °C): 5.65 (m, 1H, H^2), 4.81 (s, 5H, C_5H_5), 4.57 (d, 1H, H^4, $^2J_{HP}$ = 9.8 Hz), 3.88 (m, 1H, H^1), 3.79 (t, 1H, H^3). The resonances of coordinated PPh_3 and benzonitrile were obscured by those of both free PPh_3 and benzonitrile. After a few minutes only the resonances of **4a** and free benzonitrile were observed.

(6) Perrin, D. D.; Armarego, W. L. F. *Purification of Laboratory Chemicals*, 3rd ed.; Pergamon: New York, 1988.

Synthesis of $[Ru(\eta^5\text{-}C_5H_5)(\eta^5\text{-}C_5H_3OH\text{-}2\text{-}PBu^n_3)]CF_3SO_3$ (6a). To a solution of **2** (300 mg, 0.633 mmol) in CH_3NO_2 (5 mL), PBu^n_3 (234 μL, 0.945 mmol) was added, and the mixture was stirred for 30 min at 35 °C. The solution was evaporated to dryness, and in order to remove unreacted PBu^n_3, the solid residue was washed 3 times with diethyl ether (10 mL). The crude product was redissolved in CH_3NO_2, and undissolved materials were removed by filtration. On addition of diethyl ether, a pale yellow precipitate was formed which was collected on a glass-frit, washed with diethyl ether, and dried under vacuum. Yield: 324 mg (85.7%). Anal. Calcd for $C_{23}H_{36}F_3O_4PRuS$: C, 46.22; H, 6.07; S, 5.36. Found: C, 46.33; H, 6.16; S, 5.92. ^1H NMR (δ, CD_3CN, 20 °C): 4.93 (m, 1H), 4.70 (s, 5H, C_5H_5), 4.60 (m, 1H), 4.48 (m, 1H), 2.32−2.17 (m, 6H), 1.62−1.41 (m, 12H), 0.94 (t, 9H). $^{31}P\{^1H\}$ NMR (δ *vs* PPh_3, CD_3CN, 20 °C): 36.1.

Synthesis of $[Ru(\eta^5\text{-}C_5H_5)(\eta^5\text{-}C_5H_3OH\text{-}2\text{-}PCy_3)]CF_3SO_3$ (6b). This compound was synthesized analogously to **6a** by treatment of **2** (280 mg) with 1 equiv of PCy_3. Yield: 329 mg (82.3%). Anal. Calcd for $C_{29}H_{42}F_3O_4PRuS$: C, 51.55; H, 6.62; S, 4.64. Found: C, 51.41; H, 6.57; S, 4.70. ^1H NMR (δ, CD_3CN, 20 °C): 5.01 (m, 1H), 4.64 (s, 5H, C_5H_5), 4.63 (m, 1H), 4.50 (m, 1H), 2.65 (q, 3H), 2.18−1.03 (m, 30H). $^{31}P\{^1H\}$ NMR (δ *vs* PPh_3, CD_3CN, 20 °C): 30.3.

Synthesis of $[Ru(\eta^5\text{-}C_5H_5)(\eta^5\text{-}C_5H_3OH\text{-}2\text{-}PPhMe_2)]CF_3SO_3$ (6c). This compound was synthesized analogously to **6a** by treatment of **2** (300 mg) with 1 equiv of $PPhMe_2$. Yield: 276 mg (79.7%). Anal. Calcd for $C_{19}H_{20}F_3O_4PRuS$: C, 42.78; H, 3.78; S, 6.01. Found: C, 42.61; H, 3.80; S, 6.22. ^1H NMR (δ, CD_3CN, 20 °C): 7.82−7.78 (m, 5H), 4.86 (m, 1H), 4.62 (s, 5H, C_5H_5), 4.58 (m, 1H), 4.46 (m, 1H), 2.42 (d, 6H, J = 14.1 Hz). $^{31}P\{^1H\}$ NMR (δ *vs* PPh_3, CD_3CN, 20 °C): 32.7.

Reaction of 2 with PMe_3 in CH_3NO_2. Following the protocol for complexes **6a**−**c**, treatment of **2** (320 mg, 0.675 mmol) with PMe_3 (1.5 equiv) in CH_3NO_2 resulted in a 40/60 mixture of $[Ru(\eta^5\text{-}C_5H_5)(\eta^5\text{-}C_5H_3OH\text{-}2\text{-}PMe_3)]CF_3SO_3$ (**6d**) and $[Ru(\eta^5\text{-}C_5H_4\text{-}PMe_3)(\eta^5\text{-}C_5H_4OH)]CF_3SO_3$ (**7**). No attempts have been made to separate these complexes. Overall yield: 255 mg. NMR for **6d**: ^1H (δ, CD_3CN, 20 °C) 5.00 (m, 1H), 4.75 (m, 1H), 4.74 (s, 5H, C_5H_5), 4.62 (m, 1H), 1.98 (d, 9H, $^2J_{HP}$ = 14.4 Hz); $^{31}P\{^1H\}$ (δ *vs* PPh_3, CD_3CN, 20 °C) 26.2. **7**: ^1H NMR (δ, CD_3CN, 20 °C): 5.19 (m, 2H), 4.96 (m, 2H), 4.83 (m, 2H), 4.39 (m, 2H), 2.03 (d, 9H, $^2J_{HP}$ = 14.7 Hz).

Reaction of 2 with PMe_3 in Acetone. Formation of $[Ru(\eta^5\text{-}C_5H_4O)((1\text{-}4\text{-}\eta)\text{-}5\text{-}endo\text{-}py\text{-}C_5H_5)(PMe_3)]CF_3SO_3$ (8a). To a solution of **2** (200 mg, 0.422 mmol) in acetone (5 mL), PMe_3 (0.86 mL, 0.844 mmol) was added resulting in the immediate formation of a pale yellow precipitate which was collected on a glass-frit, washed with diethyl ether, and dried under vacuum. Yield: 230 mg (99%). Anal. Calcd for $C_{19}H_{23}F_3NO_4PRuS$: C, 41.46; H, 4.21; N, 2.54; P, 5.82. Found: C, 42.41; H, 4.30; N, 2.42; P, 5.63. ^1H NMR (δ, CD_3NO_2, 20 °C): 9.17 (m, 2H, py), 7.91 (m, 1H, py), 7.44 (m, 2H, py), 5.49 (m, 2H), 4.83 (m, 2H), 3.79 (m, 2H), 3.70 (m, 2H), 3.10 (m, 1H), 1.58 (d, 9H, $^2J_{HP}$ = 14.0 Hz). $^{31}P\{^1H\}$ NMR (δ *vs* PPh_3, CD_3CN, 20 °C): 25.1. IR (KBr, cm^{-1}): 3100 (w), 2924 (s), 2830 (m, $\nu_{C-H(exo)}$), 1593 (s, ν_{C-O}), 1480 (m), 1275 (s, CF_3SO_3), 1231 (CF_3SO_3), 1173 (s), 1048 (CF_3SO_3), 983 (m), 648 (CF_3SO_3).

Reaction of 2 with Tertiary Phosphines in Acetone-d_6. Typically a 5 mm NMR tube was charged with **2** (30 mg, 0.063 mmol) and capped with a septum. A solution of the tertiary phosphine (*ca*. 1.5 equiv) in acetone-d_6 (0.5 mL) was added by syringe, and the sample was transferred to an NMR probe. ^1H NMR spectra were immediately recorded. For PBu^n_3, the formation of intermediates $[Ru(\eta^5\text{-}C_5H_4O)\text{-}((1\text{-}4\text{-}\eta)\text{-}5\text{-}endo\text{-}py\text{-}C_5H_5)(PBu^n_3)]CF_3SO_3$ (**8b**) and $[Ru(\eta^5\text{-}C_5H_5)(\eta^3\text{-}C_5H_4O\text{-}2\text{-}PBu^n_3)(py)]CF_3SO_3$ (**9a**) was observed. NMR for **8b**: ^1H (δ, acetone-d_6, 20 °C) 9.13 (m, 2H, py), 7.90 (m, 1H, py), 7.40 (m, 2H, py), 5.61 (m, 2H), 4.86 (m, 2H), 3.88 (m, 2H), 3.85 (m, 2H), 3.16 (m, 1H). The resonances of PBu^n_3 were superimposed by those of the free phosphine. ^1H NMR for **9a** (δ, acetone-d_6, 20 °C): 9.19 (m, 1H, py), 8.33 (m, 1H, py), 7.93 (m, 1H, py), 7.45 (m, 1H, py), 7.34 (m, 1H, py), 6.00 (ddd, 1H, H^2, $^3J_{12}$ = 2.5 Hz; $^3J_{34}$ = 4.0 Hz, $^4J_{24}$ = 1.6 Hz), 4.56 (s, 5H, C_5H_5), 4.27 (m, 1H, H^1, $^3J_{12}$ = 2.5 Hz, $^4J_{13}$ = 1.2 Hz), 3.80 (ddd, 1H, H^3, $^3J_{23}$ = 4.0 Hz, $^3J_{HP}$ = 5.3 Hz, $^4J_{12}$ = 1.2 Hz), 1.90 (dd, 1H, H^4, $^2J_{HP}$ = 10.8 Hz, $^4J_{24}$ = 1.6 Hz). The resonances of PBu^n_3 were superimposed by the signals of free phosphine. After a few minutes additional resonances were observed due to the formation of

6a and liberated pyridine. For PCy_3, only the formation of [Ru(η^5-C_5H_5)(η^3-C_5H_4O-2-PCy_3)(py)]CF_3SO_3 (**9b**) was observed. ^{1}H NMR (δ, acetone-d_6, 20 °C): 9.12 (m, 1H, py), 8.33 (m, 1H, py), 7.90 (m, 1H, py), 7.45 (m, 1H, py), 7.39 (m, 1H, py), 6.00 (m, 1H, H^2), 4.59 (s, 5H, C_5H_5), 4.36 (m, 1H, H^1), 3.80 (m, 1H, H^3). The resonances of H^4 and PCy_3 were obscured by the proton resonances of free PCy_3. Additional resonances due to the formation of **6b** and free pyridine were observed after a few minutes. For $PPhMe_2$, the formation of [Ru(η^5-C_5H_5)(η^3-C_5H_4O-$PPhMe_2$)(py)]CF_3SO_3 (**9c**) was observed. ^{1}H NMR (δ, acetone-d_6, 20 °C): 9.14 (m, 1H, py), 8.33 (m, 1H, py), 7.88 (m, 1H, py), 7.72−7.66 (m, 5H, Ph), 7.49 (m, 1H, py), 7.38 (m, 1H, py), 5.81 (m, 1H, H^2), 4.59 (s, 5H, C_5H_5), 3.71 (m, 1H, H^1), 3.12 (m, 1H, H^3), 2.14 (d, 6H, J = 12.6 Hz), 1.98 (d, 1H, H^4, $^2J_{HP}$ = 10.2 Hz). Additional resonances due to the formation of **6c** and free pyridine were observed after a few minutes. For PMe_3, on addition of PMe_3 (*ca*. 1.5 equiv) in acetone-d_6 by syringe, a pale yellow precipitate was immediately formed which precluded the recording of an NMR spectrum.

Attempted Reaction of 2 with PPh_2Me, P(*p*-PhOMe)$_3$, and PPh_3. A 5 mm NMR tube was charged with **2** (30 mg, 0.063 mmol) and capped with a septum. A solution of either PPh_2Me, P(*p*-PhOMe)$_3$, or PPh_3 in acetone-d_6 (0.5 mL) was added by syringe, the sample was transferred to an NMR probe, and ^{1}H NMR spectra were recorded. After 5 days, no reaction had occurred and >97% of **2** remained.

Reaction of 2 with Tertiary Phosphines in CD_3NO_2. A 5 mm NMR tube was charged with **2** (30 mg, 0.063 mmol) and capped with a septum. A solution of either PBu^n_3, $PPhMe_2$, or PMe_3 in CD_3NO_2 (0.5 mL) was added by syringe, and the sample was transferred to an NMR probe. ^{1}H NMR spectra were immediately recorded. The poor solubility of PCy_3 in CD_3NO_2 precluded the recording of a ^{1}H NMR spectrum. The ^{1}H NMR spectra of PBu^n_3 and $PPhMe_2$ are similar to those recorded in acetone-d_6 showing the formation of intermediates **9a**−**c** and **6a**−**c**. For PMe_3, the formation of [Ru(η^5-C_5H_5)(η^3-C_5H_4O-2-PMe_3)(py)]CF_3SO_3 (**9d**) was observed. ^{1}H NMR (δ, CD_3NO_2, 20 °C): 9.03 (m, 1H, py), 8.29 (m, 1H, py), 7.93 (m, 1H, py), 7.51 (m, 1H, py), 7.26 (m, 1H, py), 5.971 (m, 1H, H^2), 4.55 (s, 5H, C_5H_5), 4.28 (m, 1H, H^1), 3.75 (m, 1H, H^3). The resonance of H^4 could not be detected. Additional resonances due to the formation of **6d**, **7**, and free pyridine were also observed.

Synthesis of [Ru(η^5-C_5H_5)(η^3-C_5H_4O-2-PBu^n_3)(tu)]CF_3SO_3 (10a). To a solution of **3** (400 mg, 0.848 mmol) in CH_3CN (7 mL), PBu^n_3 (0.315 mL, 1.273 mmol) was added, and the mixture was stirred for 10 min at room temperature whereupon a bright yellow precipitate was formed. Diethyl ether was added, and the precipitate was collected on a fritted glass funnel, washed with diethyl ether, and dried under vacuum. Yield: 440 mg (77.0%). Anal. Calcd for $C_{24}H_{40}F_3N_2O_4PRuS_2$: C, 42.79; H, 5.98; N, 4.16; S, 9.52. Found: C, 42.53; H, 5.86; N, 4.23; S, 9.44. ^{1}H NMR (δ, CD_3CN, 20 °C): 7.01 (br, 4H, NH_2), 5.63 (m, 1H, H^2), 4.63 (s, 5H, C_5H_5), 3.82 (m, 1H, H^1), 3.24 (m, 1H, H^3), 3.00 (d, 1H, H^4, $^2J_{HP}$ = 8.4 Hz), 2.02 (m, 6H), 1.45 (m, 18H), 0.92 (t, 9H). ^{31}P{^{1}H} NMR (δ *vs* PPh_3, acetone-d_6, 20 °C): 37.9. IR (poly(chlorotrifluoroethylene), cm^{-1}): 1649 (s, $\nu_{C=O}$).

Synthesis of [Ru(η^5-C_5H_5)(η^3-C_5H_4O-2-PCy_3)(tu)]CF_3SO_3 (10b). This compound was synthesized analogously to **10a** by treatment of **3** (405 mg, 0.859 mmol) with PCy_3 (361 mg). Yield: 509 mg (79.0%). Anal. Calcd for $C_{30}H_{46}F_3N_2O_4PRuS_2$: C, 47.93; H, 6.17; N, 3.73; S, 8.53. Found: C, 47.71; H, 6.07; N, 3.80; S, 8.67. ^{1}H NMR (δ, acetone-d_6, 20 °C): 7.73 (br, 4H, NH_2), 5.72 (m, 1H, H^2), 4.69 (s, 5H, C_5H_5), 3.92 (m, 1H, H^1), 3.63 (d, 1H, H^4, $^2J_{HP}$ = 11.9 Hz), 3.50 (m, 1H, H^3), 2.74 (q, 3H), 2.10−1.30 (m, 30H). ^{31}P{^{1}H} NMR (δ *vs* PPh_3, acetone-d_6, 20 °C): 41.3. IR (poly(chlorotrifluoroethylene), cm^{-1}): 1644 (s, $\nu_{C=O}$).

Synthesis of [Ru(η^5-C_5H_5)(η^3-C_5H_4O-2-$PPhMe_2$)(tu)]CF_3SO_3 (10c). This compound was synthesized analogously to **10a** by treatment of **3** (200 mg, 0.424 mmol) with $PPhMe_2$ (0.91 mL). Yield: 165 mg (64.0%). Anal. Calcd for $C_{20}H_{24}F_3N_2O_4PRuS_2$: C, 39.41; H, 3.97; N, 4.60; S, 10.52. Found: C, 39.53; H, 3.90; N, 4.77; S, 10.34. ^{1}H NMR (δ, CD_3CN, 20 °C): 7.74 (br, 4H, NH_2), 7.70−7.63 (m, 5H), 5.34 (m, 1H, H^2), 4.57 (s, 5H, C_5H_5), 3.65 (m, 1H, H^1), 3.30 (d, 1H, H^4, $^2J_{HP}$ = 7.6 Hz), 3.12 (m, 1H, H^3), 2.03 (d, 6H, $^2J_{HP}$ = 13.8 Hz). ^{31}P{^{1}H} NMR (δ *vs* PPh_3, acetone-d_6, 20 °C): 31.7. IR (poly-(chlorotrifluoroethylene), cm^{-1}): 1652 (s, $\nu_{C=O}$).

Synthesis of [Ru(η^5-C_5H_5)(η^3-C_5H_4O-2-PMe_3)(tu)]CF_3SO_3 (10d). This compound was synthesized analogously to **10a** by treatment of **3** (300 mg, 0.636 mmol) with PMe_3 (130 μL, 1.273 mmol). Yield: 201 mg (58%). Anal. Calcd for $C_{15}H_{22}F_3N_2O_4PRuS_2$: C, 32.91; H, 4.05; N, 5.12; S, 11.71. Found: C, 33.35; H, 4.12; N, 5.17; S, 11.69. ^{1}H NMR (δ, acetone-d_6, 20 °C): 7.69 (br, 4H, NH_2), 5.58 (m, 1H, H^2), 4.74 (s, 5H, C_5H_5), 4.04 (m, 1H, H^1), 3.81 (d, 1H, H^4, $^2J_{HP}$ = 9.3 Hz), 3.24 (m, 1H, H^3), 2.28 (d, 9H, $^2J_{HP}$ = 12.1 Hz). ^{31}P{^{1}H} NMR (δ *vs* PPh_3, acetone-d_6, 20 °C): 28.6. IR (poly(chlorotrifluoroethylene), cm^{-1}): 1648 (s, $\nu_{C=O}$).

Reaction of 3 with Tertiary Phosphines in CD_3NO_2. Typically a 5 mm NMR tube was charged with **3** (30 mg, 0.0636 mmol) and capped with a septum. A solution of the tertiary phosphine (*ca*. 1.5 equiv) in CD_3NO_2 (0.5 mL) was added by syringe, and the sample was transferred to an NMR probe. ^{1}H and ^{31}P{^{1}H} NMR spectra were immediately recorded. For PBu^n_3, the formation of [Ru(η^5-C_5H_4O)((1-4-η)-5-*endo*-tu-C_5H_5)(PBu^n_3)]CF_3SO_3 (**11a**) and [Ru(η^5-C_5H_5)(η^3-C_5H_4O-PBu^n_3)(tu)]CF_3SO_3 (**10a**) was observed. NMR for **11a**: ^{1}H (δ, CD_3NO_2, 20 °C) 7.63 (br, 4H, NH_2), 5.54 (m, 2H), 4.87 (m, 2H), 4.77 (m, 1H), 3.92 (m, 2H), 3.58 (m, 2H); ^{31}P{^{1}H} (δ vs PPh_3, CD_3NO_2, 20 °C) 28.7. The proton resonances of PBu^n_3 are superimposed by those of the free phosphine. Additional resonances due to the formation of **6a** and free thiourea were observed after a few minutes. For PMe_3, initially, only formation of [Ru(η^5-C_5H_4O)((1-4-η)-5-*endo*-tu-C_5H_5)(PMe_3)]CF_3SO_3 (**11b**) was observed. ^{1}H NMR (δ, CD_3NO_2, 20 °C): 7.58 (br, 4H, NH_2), 5.55 (m, 2H), 4.90 (m, 2H), 4.55 (m, 1H), 3.98 (m, 2H), 1.58 (d, 9H, $^2J_{HP}$ = 13.8 Hz). The appearance of additional resonances due to the formation of **6d**, **7**, and free thiourea was observed after a few minutes.

Reaction of 3 with Tertiary Phosphines in Acetone-d_6. A 5 mm NMR tube was charged with **3** (30 mg, 0.0636 mmol) and capped with a septum. A solution of the tertiary phosphine (*ca*. 1.5 equiv) in acetone-d_6 (0.5 mL) was added by syringe, and the sample was transferred to an NMR probe. ^{1}H NMR spectra were immediately recorded. For PBu^n_3, the formation of **10a** was observed. Additional resonances due to the formation of **6a** and free thiourea were detected after a few minutes. There was no indication of **11a** being formed. For PCy_3, the formation of **10b** was observed. After several minutes additional resonances due to the formation of **6b** and free thiourea were observed. For PMe_3, there was no evidence for the formation of either **11b**, **10d**, **6d**, or **7**; instead, the formation of several, as yet, not identified compounds was observed.

Conversion of **10a**−**d to 6a**−**d.** The reactions were performed on a scale suitable for NMR experiments. Typically, 30 mg of these respective complexes were dissolved in CD_3CN (0.5 mL). The solutions were transferred into an NMR tube and both the consumption of **10a**−**d** and the formation of **6a**−**d** were monitored by ^{1}H NMR spectroscopy at various temperatures. Peak integration was with respect to an internal CH_2Cl_2 standard.

X-ray Structure Determination for 10a. Crystal data and experimental details are given in Table 1. X-ray data were collected on a Philips PW1100 four-circle diffractometer using graphite monochromated Mo Kα (λ = 0.710 69 Å) radiation and the $\theta-2\theta$ scan technique. Three representative reference reflections were measured every 120 min and used to correct for crystal decay and system instability. Corrections for Lorentz and polarization effects were applied. The structure was solved by direct methods.[8] All non-hydrogen atoms were refined anisotropically and hydrogen atoms were included in idealized positions.[9] The structures were refined against F^2. In order to compensate for the poor counting statistics of the reflection data (small crystal), hard and soft restraints for bond lengths and U_{ij} were applied (idealized C_5H_5 ring; SADI.0001 bond length restraints for chemically equivalent bonds in allyl, PBu^n_3, thiourea, and $CF_3SO_3^-$ moieties; SIMU and DELU soft restraints for the C_5H_5, PBu^n_3, and $CF_3SO_3^-$ moieties). The final full-matrix least-squares refinement

(7) Bevington, P. R. *Data Reduction and Error Analysis for the Physical Sciences*; McGraw-Hill: New York, 1969.
(8) Hall, S. R.; Flack, H. D.; Stewart, J. M. *XTAL3.2, Integrated System of Computer Programs for Crystal Structure Determination*; Universities of Western Australia (Australia), Geneva (Switzerland), and Maryland (USA), 1992.
(9) Sheldrick, G. M. *SHELXL93, Program for Crystal Structure Refinement*; University of Göttingen: Göttingen, Germany, 1993.

Table 1. Crystallographic Data and Experimental Details[a]

formula	$C_{24}H_{40}F_3N_2O_4PRuS_2$	λ (Å)	0.71069
fw	637.74	abs corr	none
cryst size, mm	0.05 × 0.16 × 0.44	θ_{max} (deg)	25
space group	$P2_12_12_1$ (No. 19)	index ranges	$-22 \le h$ 22, $0 \le h \le 15$, $0 \le l \le 12$
a (Å)	20.039(5)	no. of reflns measd	4957
b (Å)	13.726(4)	no. of unique reflns	4357
c (Å)	11.249(3)	no. of reflns > $4\sigma(F)$	2611
V (Å^{-3})	3102(1)	no. of params	327
Z	4	$R(F)$ ($F > 4\sigma(F)$)	0.070
ρ_{calc} (g cm^{-3})	1.442	$R(F)$ (all data)	0.139
T (K)	298	$R_w(F^2)$ (all data)	0.145
μ(Mo Kα) (mm^{-1})	0.74	diff fourier peaks min/max, e Å^{-3}	−0.40/0.44

[a] $R(F) = ||F_o| - |F_c||/|F_o|$. $R_w(F^2) = [w(F_o^2 - F_c^2)^2/wF_o^4]^{0.5}$.

varied 327 parameters, applied 166 restraints, and used 4357 independent reflections. Final positional parameters for all non-hydrogen atoms are given in supporting information Table S1, positional and isotropic displacement parameters for the hydrogen atoms appear in Table S2, anisotropic displacement parameters for non-hydrogen atoms are in Table S3, a full list of bond lengths and angles is given in Table S4, and the parameters describing the least-squares planes are in Table S5.

Kinetic Studies of the Reaction between [Ru(η^5-C_5H_4O)(CH_3CN)]CF_3SO_3 (1a) and PPh_3, P(*p*-PhOMe)$_3$, and PPh_2Me in Acetone. The ambient pressure stopped-flow kinetic data were obtained with a Hi-Tech SF-40 instrument. The optical signal at 400 nm was monitored. The data were collected as sets of 2048 points, corresponding to 3−4 half-lives, using a Physical Data Model 414A digitizer and transferred to a DOS/Windows based personal computer for data analysis. For particularly slow reactions, requiring more than 500 s of data, the first 500 s of data were transferred to the computer and the digitizer was retriggered. A stopwatch was used to measure the time from mixing to the beginning of the second data set, and the data sets were combined for analysis. The data all involved pseudo-first-order conditions with the phosphine in large excess over the ruthenium complex. The data were typically biphasic, showing a rapid absorbance increase followed by a slower absorbance decrease. They were all fit to a sum of two exponentials using either or both of two different nonlinear least-squares procedures. One of the algorithms consisted of the CURFIT routine of Bevington[7] programmed in QuickBasic. The other consisted of the Scientist data analysis package.

High-pressure stopped-flow measurements were made with a Hi-Tech model HPS-2000 mixing system and the same spectrometer unit and data acquisition system as used for the ambient pressure reactions. The mixing system consists of a solenoid-powered, ratcheted drive for 2 mL glass-barreled syringes, a fused quartz cell, and a 5 mL waste syringe. The flow system components were connected by Teflon valves and tubing. This entire apparatus was placed in the pressure vessel. Light is brought in and out through sapphire windows. A Pressure Products Industries pump filled with Dow Corning 200 fluid (dimethylpolysiloxane) was used for pressurizing the stainless steel vessel. The pressure vessel is kept in a thermostated bath at 25 °C, and the internal temperature is monitored with a Pt resistance sensor. The high-pressure apparatus gives a maximum of eight shots for each filling of the syringes and pressurization of the system. Several pressures were measured for each filling.

Results and Discussion

Reactions of Tertiary Phosphines with [Ru(η^5-C_5H_5)(η^4-C_5H_4O)(py)]CF_3SO_3 (2). The tertiary phosphines PBu^n_3, PCy_3, and $PPhMe_2$ react with **2** in CH_3NO_2 to give, on workup, solely 1,2-disubstituted ruthenocenes **6a**−**c** in high yields (Scheme 2). The reaction of **2** with PMe_3 is less selective and affords a 40/60 mixture of 1,2-disubstituted and 1,1′-disubstituted ruthenocenes **6d** and **7**. By contrast, with PPh_3, P(*p*-PhOMe)$_3$, and PPh_2Me no reaction takes place, even upon prolonged stirring at room temperature. The identity of the products has been established by ^{1}H NMR spectroscopy and elemental analysis. The ^{1}H NMR spectra of **6a**−**d** are altogether similar to those of the analogous complexes [Ru(η^5-C_5H_5)(η^5-C_5H_3-OH-2-PR_3)]PF_6 (PR_3 = PPh_3 (**4a**), PPh_2Me (**4b**), P(*p*-PhOMe)$_3$ (**4c**)) reported earlier[3d] and will not be further discussed. It is interesting to note, however, that in sharp contrast to **2**, **1a** reacts with PMe_3, PBu^n_3, PCy_3, and $PPhMe_2$ exclusively to give 1,1′-disubstituted ruthenocenes.[3d]

Scheme 2

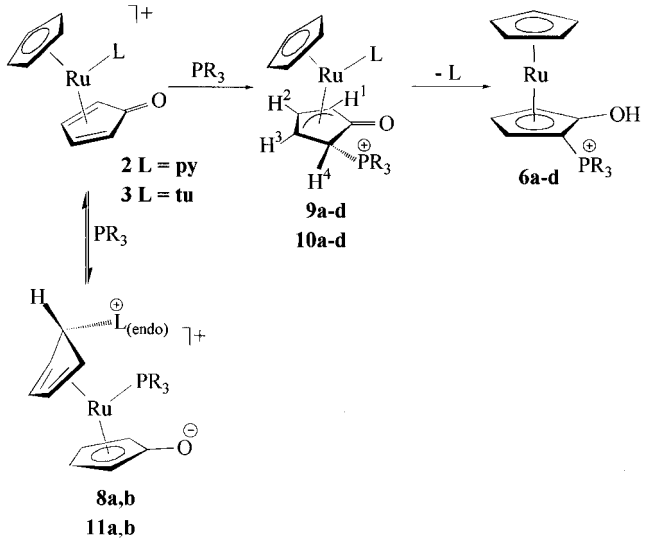

The above reactions performed in acetone as the solvent led, with the exception of PMe_3, to the same products. Addition of PMe_3 to a solution of **2** in acetone affords a pale yellow compound in essentially quantitative yield tentatively formulated as [Ru(η^5-C_5H_4O)((1−4-η)-5-*endo*-py-C_5H_5)(PMe_3)]CF_3SO_3 (**8a**) which is insoluble in this solvent (Scheme 2). In the solid state **8a** can be handled for a short period of time but decomposition occurs readily in solution (CD_3NO_2) to give a mixture of **2**, **6d**, and **7**. The proposed mechanism for the formation of **8a** involves nucleophilic attack of PMe_3 at the metal center resulting in an intramolecular migratory insertion of pyridine into the cyclopentadienyl ring. The pyridinium ligand would, therefore, be *endo* to the metal center. The ^{1}H NMR spectrum is fully consistent with a 5-pyridiniumylcyclopentadiene ligand (Figure 1). The assignment of the proton resonances was afforded by homonuclear decoupling experiments. Unfortunately, the recording of a ^{13}C{^{1}H} NMR spectrum was precluded due the instability of this complex in solution. The IR spectrum exhibits a strong C−H stretch at 2830 cm^{-1} assigned to the *exo* proton, also suggesting that the pyridinium moiety is *endo* to the metal center.[10,11] The C═O peak is shifted from 1682 cm^{-1} in **2** to

(10) (a) Khand, I. U.; Pauson, P. L.; Watts, W. E. *J. Chem. Soc. (C)* **1969**, *2024*. (b) Green, M. L. H.; Pratt, L.; Wilkinson, G. *J. Chem. Soc.* **1959**, 3753.
(11) Benfield, F. W. S.; Green, M. L. H. *J. Chem. Soc., Dalton Trans.* **1974**, 1324.

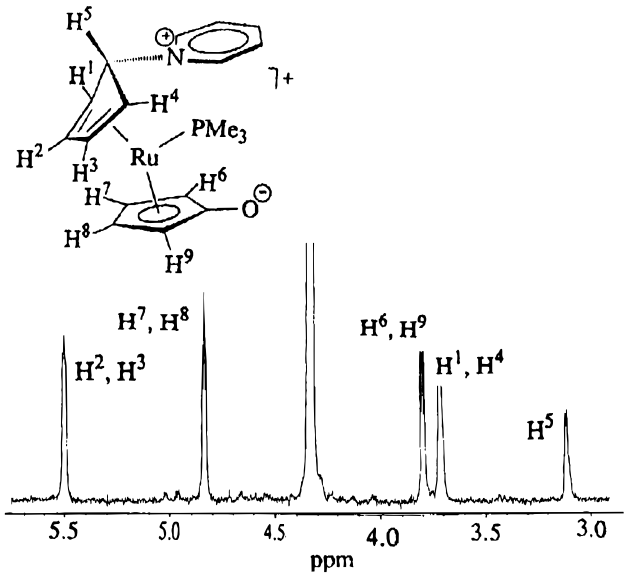

Figure 1. 250 MHz ^{1}H NMR spectrum of the polyene and polyenyl part of [Ru(η^5-C_5H_4O)((1-4-η)-5-*endo*-py-C_5H_5)(PMe_3)]CF_3SO_3 (**8a**) in CD_3NO_2.

1593 cm^{-1} in **8a**, indicating loss of π-electron density from this group to the ring and metal and, thus, a decrease in bond order. Migratory insertions into C_5H_5 rings are rare but, nevertheless, have been reported in the literature. For example, addition of PMe_3 to Mo(η^5-C_5H_5)$_2$(Et)(Cl) yields the *endo*-ethyl complex Mo(η^5-C_5H_5)((1−4-η)-5-*endo*-Et-C_5H_5)(PMe_3)(Cl).[11]

To obtain mechanistic information about the formation of **6a**−**d**, the reaction of **2** with PR_3 (PR_3 = PBu^n_3, PCy_3, $PPhMe_2$, PMe_3) was monitored by ^{1}H and ^{31}P{^{1}H} NMR spectroscopy in both acetone-d_6 and CD_3NO_2 as the solvents. This indicated two observable parallel reactions: (i) reversible nucleophilic attack of PR_3 at the metal center affords **8a** and **8b** and (ii) nucleophilic attack at the cyclopentadienone ligand to give intermediate **9a**−**d** (Scheme 2). Nucleophilic attack at the metal center, however, is observed only for the sterically less demanding yet very basic phosphines PMe_3 and PBu^n_3 yielding **8a** and **8b**, respectively. The nucleophilicity is taken to increase in the order of increasing pK_a[12] $PPhMe_2$ < PMe_3 < PBu^n_3 < PCy_3, while the bulkiness of the phosphines, as expressed by their cone angles,[13] increases in the order PMe_3 < $PPhMe_2$ < PBu^n_3 < PCy_3. Moreover, the formation of **6b** appears to be more pronounced in the more polar solvent CD_3NO_2 than in acetone-d_6.

The ^{1}H NMR spectra of **9a**−**d** all are very similar and, thus, structural evidence will be discussed mainly with reference to **9a**. The assignments of the proton resonances were aided by detailed double resonance experiments. In the ^{1}H NMR spectrum of **9a**, a sharp singlet at 4.56 ppm is observed for the C_5H_5 ring; the resonance for the central allyl proton H^2 appears as a double double doublet centered at 6.00 ppm ($^3J_{34}$ = 4.0 Hz, $^3J_{12}$ = 2.5 Hz, $^3J_2$ = 1.6 Hz). The resonances for the terminal allyl protons H^1 and H^3 appear as a multiplet and as a double double doublet centered at 4.27 ($^3J_{12}$ = 2.5 Hz, $^4J_{14}$ = 1.2 Hz) and 3.80 ppm ($^3J_{23}$ = 4.0 Hz, $^3J_{HP}$ = 5.3 Hz, $^4J_{12}$ = 1.2 Hz), respectively. The aliphatic *endo* proton H^4 gives rise to a double doublet which is unusually upfield shifted to 1.90 ppm ($^2J_{HP}$ = 10.8 Hz, $^4J_{24}$ = 1.6 Hz). For comparison, the respective resonance in **10a**−**d** gives rise to a doublet centered at 3.00 ($^2J_{HP}$ = 8.4 Hz), 3.63 ($^2J_{HP}$ = 11.9 Hz), 3.30 ($^2J_{HP}$ = 7.6 Hz), and 3.81 ($^2J_{HP}$ = 12.1 Hz) ppm, respectively. Similarly, the *endo* proton H^4 of the structurally related complexes [Mo($HBpz_3$)$(CO)_2$(η^3-C_5H_4O-PR_3)]PF_6 ($HBpz_3$ = tris(pyrazolyl)borate; PR_3 = PBu^n_3, PCy_3) gives rise to a doublet centered at 3.49 ($^2J_{HP}$ = 12.9 Hz) and 3.61 ($^2J_{HP}$ = 14.1 Hz), respectively.[14] The hydrogen atoms of the pyridine ligand are magnetically inequivalent giving rise to five multiplets centered at 9.19 (1H), 8.33 (1H), 7.93 (1H), 7.45 (1H), and 7.34 ppm (1H), being indicative of a hindered rotation of pyridine about the Ru−N axis. The resonances of the PBu^n_3 moiety are superimposed by those of the free phosphine. The ^{1}H NMR spectra of **9b**−**d** show similar features and will not be discussed here. Complexes **9**, with the exception of **9d**, are cleanly converted to **6** within a few minutes (Scheme 2).

The ^{1}H NMR spectroscopic results show that nucleophilic attack takes place exclusively at the cyclopentadienone moiety in an α-position to the ketonic functional group and from the face opposite to the metal. The *exo* conformation of **9a**−**d** in solution, as drawn in Scheme 2, is also deduced from ^{1}H NMR evidence. In this conformation H^4 is situated directly over the pyridine ring. Due to anisotropic shielding by the aromatic ring current of the pyridine ligand, the *endo* proton H^4 experiences a shift of about −1.7 ppm relative to those of the analogous thiourea complexes **10a**−**d**. Furthermore, the *exo* conformation is consistent with the hindered rotation of pyridine.

Reactions of Tertiary Phosphines with [Ru(η^5-C_5H_5)(η^4-C_5H_4O)(tu)]CF_3SO_3 (3). Treatment of **3** with PBu^n_3, PCy_3, $PPhMe_2$, and PMe_3 in CH_3CN results in the formation of the novel ruthenium(II) η^3-cyclopentenoyl complexes **10a**−**d** in high yields (Scheme 2). **10a**−**d** are bright yellow air stable solids, whereas in solution conversion to **6a**−**d** occurs within a matter of hours. Characterization of these compounds has been by elemental analyses, ^{1}H and ^{31}P{^{1}H} NMR spectroscopy, and IR spectroscopy. The structure of **10a**, as determined by X-ray crystallography, is shown in Figure 2. Selected bond lengths and angles are given in the figure caption.

The ^{1}H NMR spectra of **10a**−**d** all show the expected singlet resonances for the C_5H_5 ring appearing in the range of 4.74−4.57 ppm, while characteristic multiplet resonances assignable to the allyl ligands are observed in the expected ranges. The *endo* proton H^4 is observed as a doublet in the range of 3.00−3.81 ppm. In the IR spectra of **10a**−**d**, the stretching frequency of the ketonic carbonyl group is observed at 1649, 1644, 1652, and 1648 cm^{-1}, respectively, consistent with other cyclopentenoyl complexes.[4,5,15]

The overall reaction of **3** with tertiary phosphines, as monitored by ^{1}H NMR spectroscopy in CD_3NO_2, is similar to the reactions of **2** with tertiary phosphines proceeding via the intermediacy of η^3-cyclopentenoyl complexes and will not be further discussed. It is interesting to note, however, that with PMe_3 and to a lesser extent also with PBu^n_3, the formation of [Ru(η^5-C_5H_4O)((1-4-η)-5-*endo*-tu-C_5H_5)(PMe_3)]CF_3SO_3 (**11b**) and [Ru(η^5-C_5H_4O)((1−4-η)-5-*endo*-tu-C_5H_5)(PBu^n_3)]CF_3SO_3 (**11a**), respectively, is observed. Phosphine-promoted intramolecular migratory insertions of either thiourea or pyridine into C_5H_5 has no precedence in organometallic chemistry.

Kinetic Studies

The kinetics of the following three reactions were studied in some detail, for PR_3 = PPh_3, P(*p*-PhOMe)$_3$, and PPh_2Me (eq

(12) (a) Golovin, M. N.; Rahman, Md. M.; Belemonte, J. E.; Giering, W. P. *Organometallics* **1985**, *4* 1981. (b) Bush, R. C.; Angelici, R. J. *Inorg. Chem.* **1988**, *27*, 681.

(13) Tolman, C. A. *Chem. Rev.* **1977**, *77*, 313.

(14) Slugovc, C.; Mauthner, K.; Mereiter, K.; Schmid, R.; Kirchner, K. *Organometllics* **1996**, *15*, 2954.

(15) (a) Kirchner, K.; Mereiter, K.; Schmid, R. *J. Chem. Soc., Chem. Commun.* **1994**, 161. (b) Kirchner, K.; Mereiter, K.; Umfahrer, A.; Schmid, R. *Organometallics* **1994**, *13*, 1886.

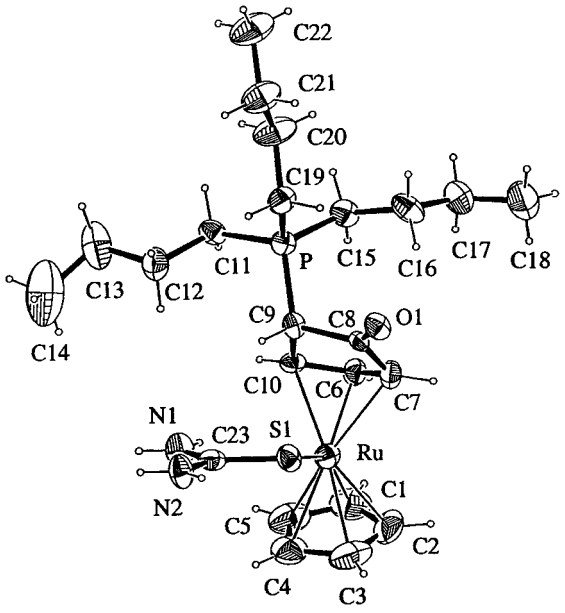

Figure 2. Structural view of $[Ru(\eta^5\text{-}C_5H_5)(\eta^3\text{-}C_5H_4O\text{-}2\text{-}PBu^n{}_3)(tu)]CF_3SO_3$ (**10a**). Selected bond lengths (Å) and angles (deg) are as follows: Ru−S(1), 2.394(4); Ru−C(7), 2.226(11); Ru−C(6), 2.054(11); Ru−C(10), 2.181(10); Ru−C(1−5)$_{av}$, 2.199(10); C(8)−O(1), 1.219(13); C(9)−P, 1.810(5); S(1)−C(23), 1.694(13); C(23)−N(1), 1.333(9); C(7)−C(6)−C(10), 106.6(10); Ru−S(1)−C(23), 110.2(3); C(7)−C(8)−C(9), 105.4(10).

1), and with acetone as the solvent. The reaction with PR_3 =

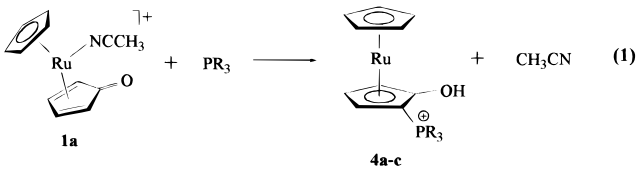

PPh_3 was studied for triphenylphosphine concentrations from 0.030 to 0.848 M and temperatures from 10 to 50 °C. A total of 145 data sets representing 49 different conditions of temperature and phosphine concentration were obtained and analyzed. The reaction with $PR_3 = P(p\text{-PhOMe})_3$ was studied for phosphine concentrations from 5.1 to 120 mM and temperatures from 10 to 50 °C. A total of 121 data sets representing 44 different conditions of temperature and phosphine concentration were obtained and analyzed. In addition, the pressure dependence of the reaction with $PR_3 = P(p\text{-PhOMe})_3$ was studied for nine pressures (0.1−150 MPa) and seven phosphine concentrations (5−120 mM) at 25 °C. A total of 148 data sets representing 61 different conditions of pressure and phosphine concentration were obtained and analyzed. For the reaction with PPh_2Me, phosphine concentrations ranged from 5.7 to 95.3 mM and temperatures from 15 to 50 °C. A total of 118 data sets representing 39 different conditions were studied. In all cases, the absorbance *vs* time data fit well to a sum of two exponentials, a faster process accompanied by an absorbance increase and a slower one which led to complete bleaching of the absorbance. This gave two apparent rate constants and two amplitudes for each data set. An example of the data and the fit to it is given in Figure 3. The trends in the amplitude ratio and apparent rate constants were fit according to the following mechanism (eq 2).

This mechanism predicts two apparent rate constants, λ_1 and λ_2, with their corresponding amplitudes A_1 and A_2. These parameters can be expressed in terms of the rate constants of the mechanism, the extinction coefficient at 400 nm for **1a**, ϵ_{1a},

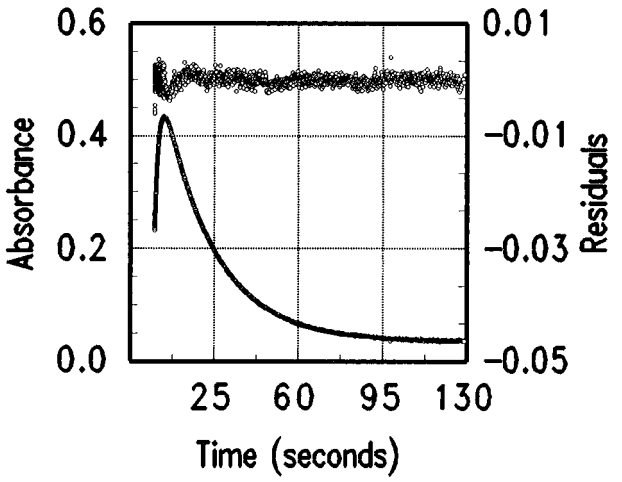

Figure 3. Absorbance *vs* time data (left abscissa) at 400 nm for the reaction of **1a** with 0.48 M PPh_3 at 35 °C. The data at the top (○) are the residuals (right abscissa) between the fit curve and the data, expanded 10-fold. The fit parameters are apparent rate constants of 4.8×10^{-2} and 0.55 s^{-1} and amplitudes of 0.53 and −0.34, respectively, with an infinite time absorbance of 0.036.

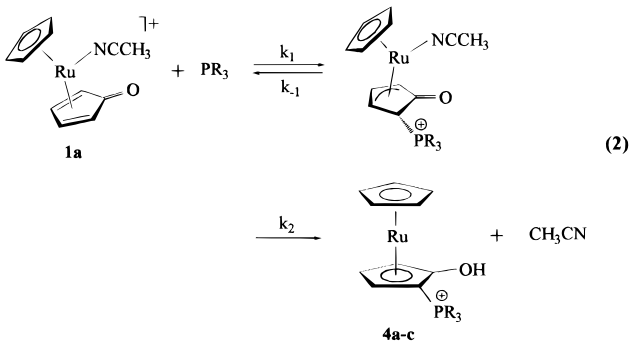

and the extinction coefficient of the intermediate, ϵ_{in} (eqs 3−7).[16]

$$p = k_1[PR_3] + k_{-1} + k_2 \tag{3}$$

$$q = (p^2 - 4k_1[PR_3]k_2)^{1/2} \tag{4}$$

$$\lambda_1 = 0.5(p + q) \tag{5}$$

$$\lambda_2 = 0.5(p - q) \tag{6}$$

$$\frac{A_1}{A_2} = \left\{\left(\frac{\lambda_1 - k_2}{\lambda_1}\right) - \left(\frac{\epsilon_{int}}{\epsilon_{1a}}\right)\right\} \Big/ \left\{\left(\frac{\epsilon_{int}}{\epsilon_{1a}}\right) - \left(\frac{\lambda_2 - k_2}{\lambda_2}\right)\right\} \tag{7}$$

The amplitude ratio was used in the fitting process in order to eliminate the need to normalize the data for the slight changes in the initial concentration of the ruthenium complex. The extinction coefficients are assumed to be temperature independent, and the temperature dependence of the rate constants is given by the Eyring equation (eq 8)

$$k_i = (k_B T/h)(\exp(-(\Delta H_i^{\ddagger} - T\Delta S_i^{\ddagger})/RT) \tag{8}$$

where k_B is the Boltzmann constant, R is the gas constant, h is Planck's constant, and T is the absolute temperature. The pressure dependence of the rate constants is also expressed by the Eyring form (eq 9)

(16) Espenson, J. H. *Chemical Kinetics and Reaction Mechanisms*; McGraw-Hill Book Company: New York, 1981.

$$k_i = k_{0,i} \exp(-\Delta V_i^{\ddagger}/RT) \quad (9)$$

where k_0 is the rate constant at ambient pressure, 0.1 MPa. The results of fitting the two sets of temperature and concentration dependent apparent rate constants are given in Table 2. The fit of the pressure and concentration dependent data gave $\Delta V_1^{\ddagger}$ of -2 ± 2 cm^3 mol^{-1}, $V_{-1}^{\ddagger}$ of -18 ± 2 cm^3 mol^{-1}, and $\Delta V_2^{\ddagger}$ of 8 ± 2 cm^3 mol^{-1}.

The quality of the fit is demonstrated by Figure 4, which shows an example of a subset of the P(*p*-PhOMe)$_3$ data at 30 °C. This demonstrates the nonlinear dependence of the two apparent rate constants on phosphine concentration and the complex variation of the amplitude ratio. The fit lines are derived from the analysis of all of the data and reproduce the kinetic behavior well. Figures S1-S4 are available as supporting information and depict the concentration and temperature dependence data for the P(*p*-PhOMe)$_3$, PPh_3, and PPh_2Me reactions and the pressure dependence data for the P(*p*-PhOMe)$_3$ reaction. All data are also available as supporting information (Tables S6-S9), with the conditions for each reaction, the observed and calculated apparent rate constants, and the amplitude ratios. The temperature dependence data are of significantly higher quality than the pressure dependence data. The origin of the scatter in the high-pressure data has not been established.

The proposed mechanism is strongly supported by the ^{1}H NMR measurements and the crystallography, as well as by conformity with the rate law. The reaction of **1a** and **1b** with PPh_3, as monitored by ^{1}H NMR spectroscopy, shows the occurrence of an intermediate where the nitrile ligand is still attached to the metal center. In the case of **1b**, this intermediate has been unequivocally identified as the η^3-cyclopentoyl complex [Ru(η^5-C_5H_5)(η^3-C_5H_4O-2-PPh_3)(bn)]$^+$. The characteristic resonances of the cyclopentenoyl moiety give rise to three multiplets centered at 5.65, 3.88, and 3.79 ppm while the *endo* proton appears as a doublet centered at 4.75 ppm with $^2J_{HP} = 9.8$ Hz. The resonance of the C_5H_5 ring appears as a singlet at 4.81 ppm. The resonances of the nitrile were superimposed by those of the PPh_3 ligand.

When the nitrile ligand is replaced by thiourea, the reactivity is decreased and the trialkylphosphines attack the C_5H_4O ring. Reaction with PBu^n_3 leads to an isolabel intermediate, [Ru(η^5-C_5H_5)(η^3-C_5H_4O-PBu^n_3)(tu)]CF_3SO_3 (**10a**), which has been characterized crystallographically. The kinetics of the conversion of **10a**−**d** to **6a**−**d**, analogous to step 2 in eq 2, has been studied by ^{1}H NMR spectroscopy in CD_3CN as a function of temperature. First-order rate constants at 25 °C and activation parameters are given in Table 3. The rate constants and activation parameters are essentially independent of the phosphine substituent.

The thermal activation parameters show a consistent pattern. The bimolecular first step, k_1, has a large negative entropy, and the last step, k_2, involving the release of CH_3CN, has a large positive entropy. The reverse of the first step, k_{-1}, shows a near zero activation entropy, indicating that the transition state still has a significant interaction with the outgoing phosphine or that there are compensating rearrangements of the η^4-C_5H_4O which make a negative contribution to the entropy of activation, balancing the positive contribution from phosphine release. The activation parameters for k_1 and k_{-1} can be combined to give the equilibrium constant, and its associated enthalpy and entropy, for the formation of the intermediate from the reactants. These values are shown in Table 2. In all cases the reaction favors the formation of the intermediate at room temperature with the more basic phosphines leading to a more thermodynamically stable compound. The highly favorable enthalpy of reaction overcomes the unfavorable entropy contribution.

Table 2. Activation Parameters and Rate Constants at 25 °C for the Reaction of [Ru(η^5-C_5H_5)(η^4-C_5H_O)(CH_3CN)]CF_3SO_3 (**1a**) with Tertiary Phosphines in Acetone

phosphine	parameter	$\Delta H^{\ddagger}$ or ΔH° (kcal mol^{-1})	$\Delta S^{\ddagger}$ or ΔS° (cal mol^{-1} K^{-1})	k^c or K
PPh_3[a]	k_1	11.6 ± 0.1	-22.5 ± 0.5	0.22 M^{-1} s^{-1}
	k_{-1}	20.6 ± 0.1	5.3 ± 0.4	0.074 s^{-1}
	k_2	23.7 ± 0.2	13.9 ± 0.5	0.029 s^{-1}
	K_1[d]	−9.0	−27.8	3.3 M^{-1}
P(*p*-PhOMe)$_3$[a]	k_1	11.6 ± 0.1	-18.6 ± 0.2	1.70 M^{-1} s^{-1}
	k_{-1}	20.9 ± 0.4	0.9 ± 1.0	0.0042 s^{-1}
	k_2	23.3 ± 0.1	13.6 ± 0.2	0.050 s^{-1}
	K_1[d]	−9.3	−19.5	350 M^{-1}
PPh_2Me[b]	k_1	13.1 ± 0.1	-13.9 ± 0.5	1.40 M^{-1} s^{-1}
	k_{-1}	23.4 ± 0.5	9.7 ± 1.7	0.0061 s^{-1}
	k_2	21.3 ± 0.2	6.1 ± 0.6	0.032 s^{-1}
	K_1[d]	−10.3	−23.6	250 M^{-1}

[a] The ratio of the extinction coefficients, $\epsilon_{Int}/\epsilon_{1a}$, is 4.2. [b] The ratio of the extinction coefficients, $\epsilon_{Int}/\epsilon_{1a}$, is 3.2. [c] Calculated from the activation parameters. [d] Calculated from k_1 and k_{-1}.

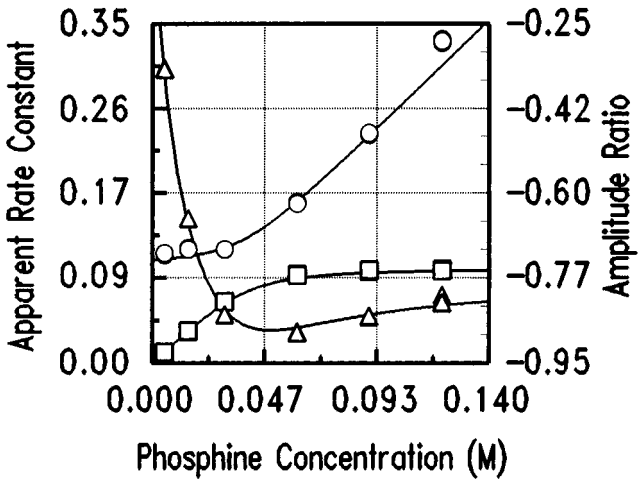

Figure 4. Dependence of the biexponential fit parameters on concentration of phosphine for the reaction of **1a** with P(*p*-PhOMe)$_3$ at 30 °C. The lower rate constant, λ_1 (□), and the higher rate constant, λ_2 (○), are plotted against the left abscissa, and the amplitude ratio, A_1/A_2 (△), is plotted against the right abscissa. Each parameter at each concentration is presented in triplicate. The solid lines are calculated from the fit to all of the data, using the parameters in Table 2.

Table 3. Activation Parameters and Observed First-order Rate Constants at 25 °C for the Conversion of [Ru(η^5-C_5H_5)(η^3-C_5H_4O-2-PR_3)(tu)]CF_3SO_3 (**10a**−**d**) to [Ru(η^5-C_5H_5)(η^5-C_5H_3OH-2-PR_3)]CF_3SO_3 (**6a**−**d**) in CD_3CN

conversion	no. of pts	T range (±1), °C	$\Delta H^{\ddagger}$ (kcal mol^{-1})	$\Delta S^{\ddagger}$ (cal mol^{-1} K^{-1})	$10^5 k_2$ (s^{-1})
19a → **6a**	11	23−60	28.0 ± 0.8	15.4 ± 0.6	4.12 ± 0.2
10b → **6b**	12	26−60	28.3 ± 0.8	15.4 ± 0.7	2.67 ± 0.1
10c → **6c**	12	25−60	27.4 ± 0.8	12.8 ± 0.5	3.05 ± 0.1
10d → **6d**	13	26−60	27.7 ± 0.8	12.5 ± 0.5	1.73 ± 0.1

Further corroboration of the mechanism comes from the data on the k_2 step as monitored by ^{1}H NMR spectroscopy. The data in Table 2 are quite consistent with those in Table 3. The entropy change is 14 ± 2 cal mol^{-1} K^{-1} for all six measurements. The slower reactions involving **3** all have $\Delta H^{\ddagger}$ values about 4 kcal mol^{-1} higher. This could very well come from the stronger bonding of thiourea to the metal center compared to CH_3CN and might also include some solvent effect since the NMR studies were done in CD_3CN instead of acetone. The k_2 data from the reaction of **1a** with PPh_2Me show significantly smaller entropy and enthalpy of activation. Compensating

effects lead to a room temperature rate constant that is quite similar to that of the other two phosphines in Table 2. This leads us to believe that there is little significant difference in the PPh_2Me reaction. The volume of activation data indicates that there is relatively little change during the k_1 step, but a large negative change during the k_{-1} step. These two values can be combined to give the difference in molar volume of 17 $cm^3\ mol^{-1}$ between the η^3-cyclopentenoyl intermediate and the reactants. This is somewhat puzzling since bond formation has occurred, but may be the result of the loosening of the η^4-C_5H_4O ring due to the shift to η^3 coordination in the intermediate state. The driving force of this reaction is presumably the stabilization energy of the aromatic ring.

Conclusions

This study has established the important details of the mechanism by which phosphines attack a coordinated C_5H_4O ring, to produce a coordinated η^5-C_5H_3OH-2-PR_3, including detailed kinetic parameters. These values and patterns will form the basis for the next steps in the study of these reactions. The first priority is to study the reactions which lead to substitution by phosphines on the C_5H_5 ring rather than at the C_5H_4O ring. We have established that this is a function of the basicity of the entering phosphine and the identity of the monodentate leaving group. When the monodentate ligand is acetonitrile or benzonitrile, only phosphines with a pK_a of greater than 5 substitute on the C_5H_5 ring. This selectivity must be a result of kinetic control since the more basic phosphines are reactive enough to attack the C_5H_4O ring, as shown by the studies in which the monodentate ligand is changed. When the leaving group is pyridine or thiourea, the two rings are deactivated such that only the C_5H_4O ring reacts, and it only reacts with the most basic phosphines. In some of these cases an intermediate has been observed in which the monodentate ligand has migrated to the C_5H_5 ring while the entering nucleophile is coordinated to ruthenium. This intermediate is formed reversibly and the products obtained still involve substitution of the phosphine only on the C_5H_4O ring.

Acknowledgment. Financial support by the "Fonds zur Förderung der wissenschaftlichen Forschung" is gratefully acknowledged (Project No. 11182).

Supporting Information Available: Kinetic data that include Figures S1−S4 showing the quality of the fit to the kinetic data as plots of calculated *vs* observed rate constants and amplitude ratios, as well as Tables S6−S9, which list the conditions and all of the measured rate constants and amplitude ratios as well as the fit values and tables of crystallographic data that include listings of all atomic positional and isotropic displacement parameters, anisotropic temeperature factors, complete bond lengths and angles, and least-squares planes for complex **10a** (Tables S1−S5) (30 pages). Ordering information is given on any current masthead page.

IC960383V